Investigation of optimum wire pitch distance in an electrostatic precipitator with multiple wire electrodes

貴島 勇希・田村 亮太・保坂 華穂・安本 浩二・川田 吉弘・瑞慶覧 章朝

［研究論文］

Investigation of optimum wire pitch distance in an electrostatic precipitator with multiple wire electrodes

Yuki KIJIMA[1], Ryota TAMURA[1], Kaho HOSAKA[1], Koji YASUMOTO[1], Yoshihiro KAWADA[2], Akinori ZUKERAN[1]

1 Dept. of Electrical and Electronic Engineering, Kanagawa Institute of Technology, Japan
2 Dept. of Electrical Environmental Energy Engineering Unit, Polytechnic University of Japan, Japan

Abstract

The purpose of this study is to show an optimum wire pitch length in an electrostatic precipitator (ESP) with multiple wire electrodes at the same energy consumption. The ESP in this study has wires-and-plates configuration. The gap length between the wire electrode and the grounded plate electrode was 15 mm. The grounded plate electrode length was 150 mm, and the wire pitch distance was between 10 and 70 mm. The particle charge considering the spatial electric field and the ion density, and the time-dependent particle trajectory were simulated. In addition, the collection efficiency was calculated whereby the optimum wire pitch was investigated at the same energy consumption. In the experiment, the collection efficiency as a function of the wire pitch was measured, and compared to the simulated result. As a result, it was revealed that the optimum pitch distance between wires was 50 mm which was approximately 3.2 times the gap length between the wire electrode and the grounded plate electrode.

Keywords: optimum wire pitch, simulation, energy efficiency, collection efficiency, electrostatic precipitator

1. Introduction

An electrostatic precipitator (ESP) has been extensively used for purifying air in houses and road tunnels, or emission gas from power plants and stealworkses, etc. Their power consumption affects CO_2 emission and fossil-fuel consumption, so the energy saving of an ESP becomes more important. The main factor of the power consumption is the use of corona discharge for charging particles in an ESP. Therefore, studies and developments on a control [1 - 3], a high voltage power supply [4], particle charging technique [5 - 6] or structure of an ESP have proceeded.

Regarding the investigation of a structure, Isahaya et al. investigated the calculation method of a corona discharge current in a multiple wire electrode type ESP [7]. Deguchi et al. concluded that the maximum corona discharge current was obtained at the pitch length between wires of 1.6 times the gap length between wire and grounded plate electrode [8]. Hamouz et al. investigated the corona discharge current density distribution on the grounded plated electrode as a function of the wire pitch length, and indicated that the distribution was influenced by the pitch length [9]. Xu et al. showed that the peak value of the discharge current density distribution was the maximum at the pitch greater than 2.7 times the gap distance [10]. Although the relationship between the corona discharge current and the pitch length was investigated by many researchers, there are few pieces of literatures describing the energy efficiency. Kawada investigated the suitable grounded plate electrode length in a single wire-to-plate type ESP at the same energy consumption, and concluded that the optimal grounded electrode length is approximately three times the gap distance [11]. Tamura et al. compared the collection efficiency in an ESP with single wire electrode with that in an ESP with three wire electrodes at the same energy consumption. As a result, it was revealed that the energy efficiency in the ESP with three wire electrode was higher than that with single wire electrode [12]. However, the influence of the pitch length on the collection efficiency at the same energy consumption in the ESP with multiple wire electrodes was not investigated.

On the other hand, Zukeran and Kawada et al. have simulated a particle charge and a charged particle trajectory in a gas flow considering the ionic flow in an ESP with a single wire electrode and three wire electrodes, and measured the particle trajectory using a particle image velocimetry (PIV) [12 – 14]. In that study, the analyzed corona current was fitted to the experimental value, whereby the negative ion density on the surface of the wire electrodes as a boundary condition was determined. The analysis current density distribution on the surface of the grounded plate electrode agreed with the experimental result using PIV.

Therefore, the purpose of this study is to show an optimum wire pitch length in an ESP with multiple wire electrodes at the same energy consumption using the above simulation method. The gap length between the wire electrode and the grounded plate electrode was 15 mm. The grounded plate electrode length was 150 mm, and the wire pitch length was between 10 and 70 mm. The

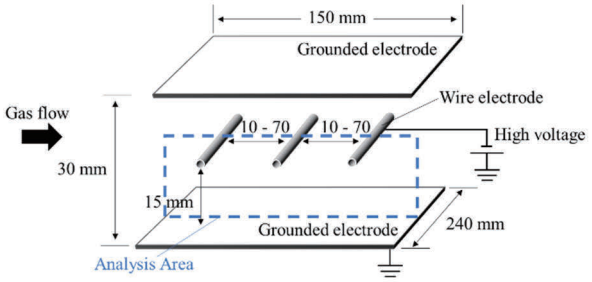

a) Electrode structure of ESP

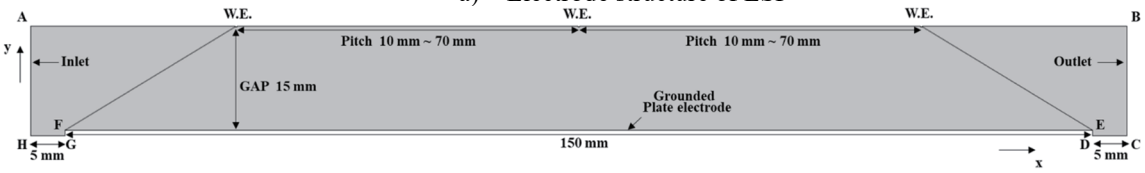

b) Analysis model

Fig. 1 ESP structure and analysis model.

Table 1 Analysis parameters.

Pitch length between wires	10 mm	30 mm	50 mm	70 mm
Corona discharge power	6 W	6 W	6 W	6 W
Applied voltage to wire electrode	-11.053 kV	-9.930 kV	-9.746 kV	-10.063 kV
Negative ion density on the surface of the wire electrode at the center of ESP	2.545×10^{14} 1/m^3	2.486×10^{15} 1/m^3	2.831×10^{15} 1/m^3	3.726×10^{15} 1/m^3
Negative ion density on the surface of the wire electrode at the inlet/outlet of ESP	3.893×10^{15} 1/m^3	2.938×10^{15} 1/m^3	2.793×10^{15} 1/m^3	2.332×10^{15} 1/m^3
Analysis corona current from the wire at the center of ESP	0.017 mA	0.181 mA	0.205 mA	0.264 mA
Analysis corona current from the wire at the inlet/outlet of ESP	0.262 mA	0.212 mA	0.206 mA	0.166 mA
Experimental corona current from the wire at the center of ESP	0.017 mA	0.180 mA	0.204 mA	0.265 mA
Experimental corona current from the wire at the inlet/outlet of ESP	0.263 mA	0.212 mA	0.207 mA	0.166 mA

particle charge and the particle trajectory were simulated. And, the collection efficiency was calculated whereby the optimum wire pitch was investigated. In the experiment, the collection efficiency as a function of the wire pitch was measured, and compared to the simulated result.

2. Simulation Methodology

The ESP structure and the analysis model for simulation is shown in Fig. 1. The ESP configuration used in this experiment is shown in Fig. 1-a. The ESP was wire-to-plate configuration which had three wire electrodes (Tungsten, $\phi = 0.26$ mm) and two grounded plate electrodes (Aluminum, t = 0.8 mm, Length: 150 mm, Width: 240 mm). The gap length between the wire electrode and the grounded plate electrode was 15 mm, and the pitch length between wire electrodes was between 10 and 70 mm. The two-dimensional space charge density distribution, electric field distribution, gas flow, particle charge considering the spatial electric field and the ion density and time-dependent particle trajectory were calculated using COMSOL Multiphysics® (Ver. 5.4). The analysis domain was the area indicated by the dashed line in Fig. 1-a, and the 2D analysis model was created as Fig. 1-b. The analysis domain was discretized into approximately 2,900,000 tetra meshes. The specific boundary conditions in Fig. 1-b are as follows:

1) Line A-B: axisymmetric boundary
2) Line B-C: outlet boundary
3) Lines C-D-E-F-G-H: wall boundary
4) Line H-A: inlet boundary
5) Line D-E-F-G: 0 V
6) Surface of wire electrode: between DC - 9.930 kV and DC -11.053 kV

The gas velocity distribution as the inlet boundary condition was determined by the result measured in the previous study [14], which was approximately 1 m/s. The analysis parameter is shown in Table 1. The voltage was determined from the experimental value at the discharge power of 6 W at each pitch length. It has already been clarified that the negative ion density on the surface of the wire electrode as the boundary condition can be determined by fitting the analyzed corona current to the experimental value [14]. Thus, the ion density in this study was determined by the same method. The analysis discharge current agreed with the experimental value as shown in Table 1.

The potential, the electric field intensity and the negative ion density were calculated by coupled analysis of Poison's and current-continuity equations as shown in reference [14]. The gas flow considering the ionic flow was calculated by the k-ω turbulence flow model. 100 particles, whose diameter was 1.5 μm, were flowed from the A-H boundary to investigate the particle trajectory and the effect of the pitch length on the collection efficiency at the same discharge power. The particle charge was calculated from the differential equations of the field and diffusion charging equations, and the charged particle trajectory was calculated by equation of motion of particles considering the gravity force, the fluid drag force and Coulomb force as described in reference [14]. The collection efficiency was calculated by counting the particles which reached the surface of the grounded plate electrode at each pitch length between 10 mm and 70 mm as shown in equation (1).

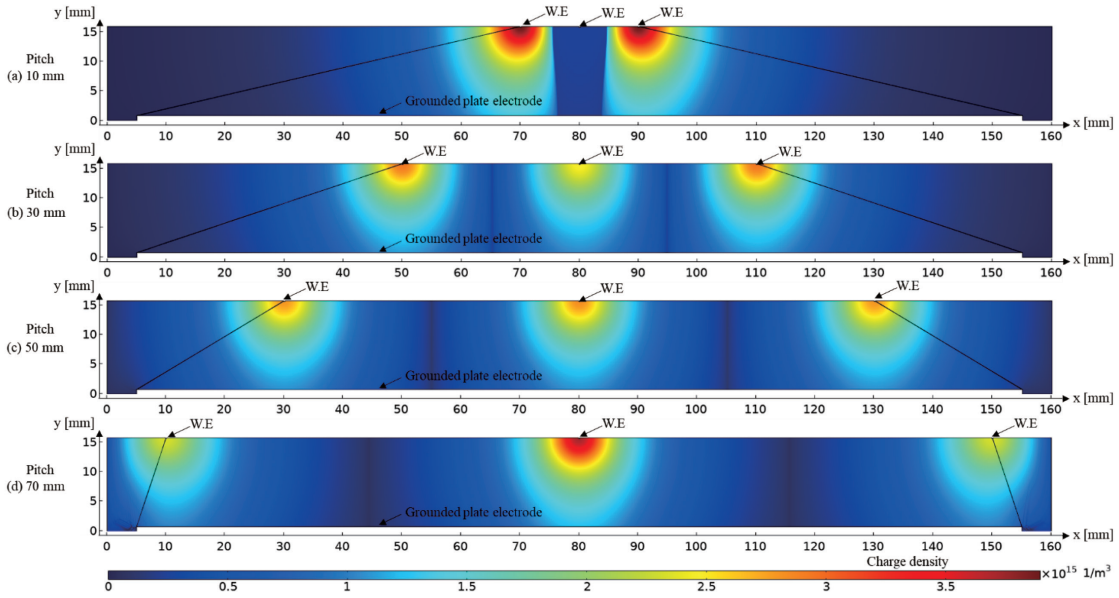

Fig. 3 Negative ion density distribution at each pitch length.

$$\eta_r = \frac{N_g}{N_i} \quad (1)$$

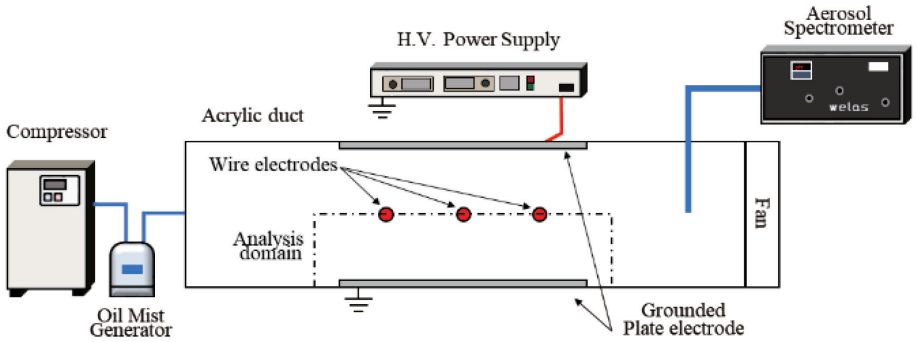

Fig. 2 Schematic diagaram of experimental system.

where, N_i is the number of particles [parts] at the inlet, N_g is the number of particles [parts] reached on the surface of the grounded plate electrode.

3. Experimental setup

The schematic diagram of experimental system is shown in Fig. 2. The electrode structure of the ESP is as shown in Fig. 1-a. The applied voltage and the discharge current were as shown in Table 1. The maximum negative high voltage of 11.053 kV was applied to the wire electrodes as the corona discharge power became 6 W. The oil mist (Junsei Chemical Co., Ltd., Olive oil) generated using an oil mist generator (Flowtech Research Inc., type: FtrOMG, nominal diameter: 1.5 μm) and a compressor mixed with the air was flowed into the ESP at the gas velocity of approximately 1 m/s. A part of the gas flow was sucked from the downstream side of the ESP, and the particle concentration for the size of 1.5 μm was measured using an aerosol spectrometer (Palas, Welas 2000). The collection efficiency was calculated using equation (2).

$$\eta = \left(1 - \frac{N_p}{N_0}\right) \times 100\% \quad (2)$$

where, N_0 is the particle concentration [parts/m^3] at the downstream end of the ESP with the applied power of 0 W, N_p is the particle concentration [parts/m^3] at the downstream end of the ESP at the applied power of 6 W.

4. Results and Discussion

4.1 Space charge density distribution

The negative ion density distribution at each pitch is shown in Fig. 3. In Fig. 3-a, the corona discharge current flowed out from the center wire electrode was low in the pitch length of 10 mm as shown in Table 1, whereby the negative ion density was low at the location x of 80 mm. The ion density at the location x of 80 mm increased with increasing the pitch due to the increase of corona discharge current at the center wire, and the distribution became uniformly at the pitch of 50 mm. Since the currents on the wires at the inlet and outlet of ESP decreased, the ion density at the center of the grounded electrode increased at the pitch length of 70 mm. The average ion density in the pitch of 10 mm, 30 mm, 50 mm and 70 mm were 5.87×10^{14} 1/m^3, 7.68×10^{14} 1/m^3, 8.51×10^{14} 1/m^3 and 7.98×10^{14} 1/m^3, respectively. The density in the pitch of 50 mm was the highest value.

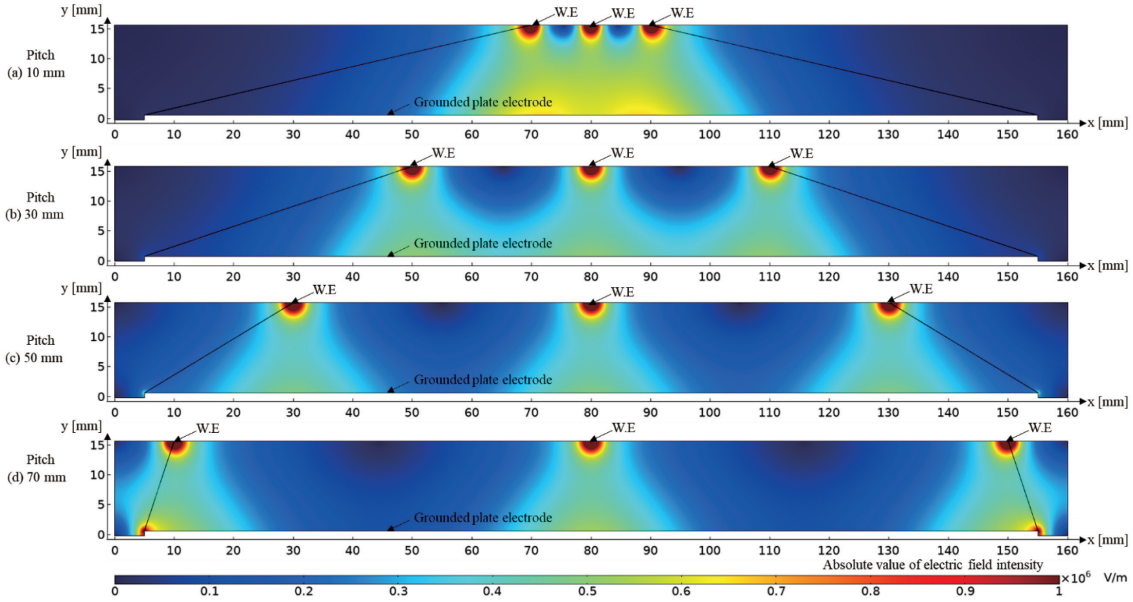

Fig. 4 Electric field intensity distribution at each pitch length.

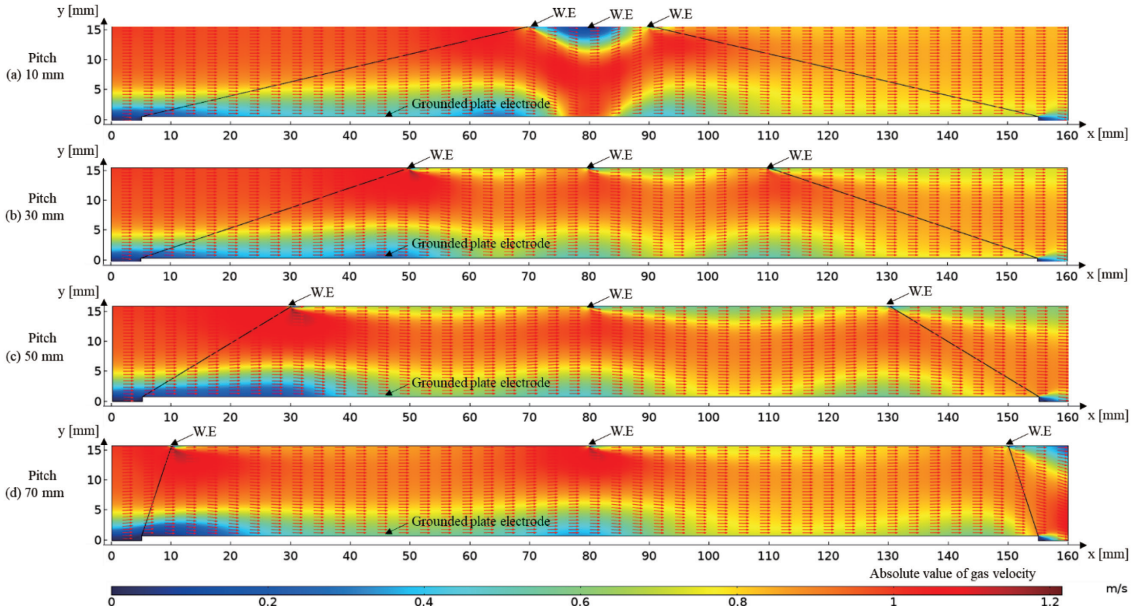

Fig. 5 Gas velocity distribution at each pitch length.

4.2 Electric field distribution

The electric field distribution at each pitch length is shown in Fig. 4. The electric field intensities were high near the wires, and these were low around the center between the wire electrode and the grounded plate electrode at any pitch lengths. The electric field intensities increased again near the surface of the grounded plate electrode due to the space charge effect. The electric field intensity distribution was uniformly in the calculation space at the pitch of 50 mm. The electric field distribution at the inlet and outlet of the ESP were distorted at the pitch of 70 mm, and the intensity at the upstream and downstream edges on the grounded plate electrode increased. The average electric field intensity in the pitch of 10 mm, 30 mm, 50 mm and 70 mm were 1.92×10^5 V/m, 2.29×10^5 V/m, 2.48×10^5 V/m and 2.39×10^5 V/m, respectively. The intensity in the pitch of 50 mm was the highest value.

4.3 Gas velocity distribution

The gas velocity distribution considering the ionic flow at each pitch length is shown in Fig. 5. The color bar indicates the absolute value of the gas velocity, and allows are the direction of gas flow. While the inlet gas velocity at the location (x, y) = (0, 0) was the lowest, that was uniformly with increasing the x value. In addition, the velocity around the wire electrodes increased and that on the surface of the grounded plate electrode under the wire electrodes decreased. These are due to the ionic flow.

4.4 Particle charge and trajectory

The particle charge and trajectory, when 100 particles are flowed in the gas velocity distribution as shown in Fig. 5, is shown in Fig. 6. The particle size is 1.5 μm. The color bar indicates the particle charge amount, and lines are the particle trajectories. All particles were charged due to the influence of the negative ion density distribution as shown in Fig. 3, and these flowed to downstream side with migrating forward to the grounded plate electrode due to the electric field distribution as shown in Fig. 4. The average of the particle charge amount, which emitted to the downstream side (x = 160 mm), at the pitch length of 10 mm, 30 mm, 50 mm and 70 mm were 8.27×10^{-17} C, 7.56×10^{-17} C, 7.46×10^{-17} C and 7.84×10^{-17} C, respectively. The average charge amount at the pitch length of 10 mm was the highest, and that of 50 mm was the lowest. Although the charge amount at 10 mm was the highest, Coulomb force was low due to the low electric field intensity at the location x greater than approximately 110 mm as shown in Fig. 4, whereby the charged particles emitted from the ESP. Since the electric field intensity at the downstream edge of the grounded plate electrode at the pitch length of 70 mm were high as described above, a part of particles was strongly charged. Due to this effect, the average particle charge amount at the pitch length of 70 mm was greater than that at 50 mm. Although the charge amount was high, these particles were not collected and emitted from the ESP.

4.5 Particle velocity and trajectory

The particle velocity and trajectory is shown in Fig. 7. The color bar indicates the absolute value of the particle velocity, and the line is the particle trajectories as the same to Fig. 6. The particle velocity around the wires increased, and that on the surface of the grounded electrode under the

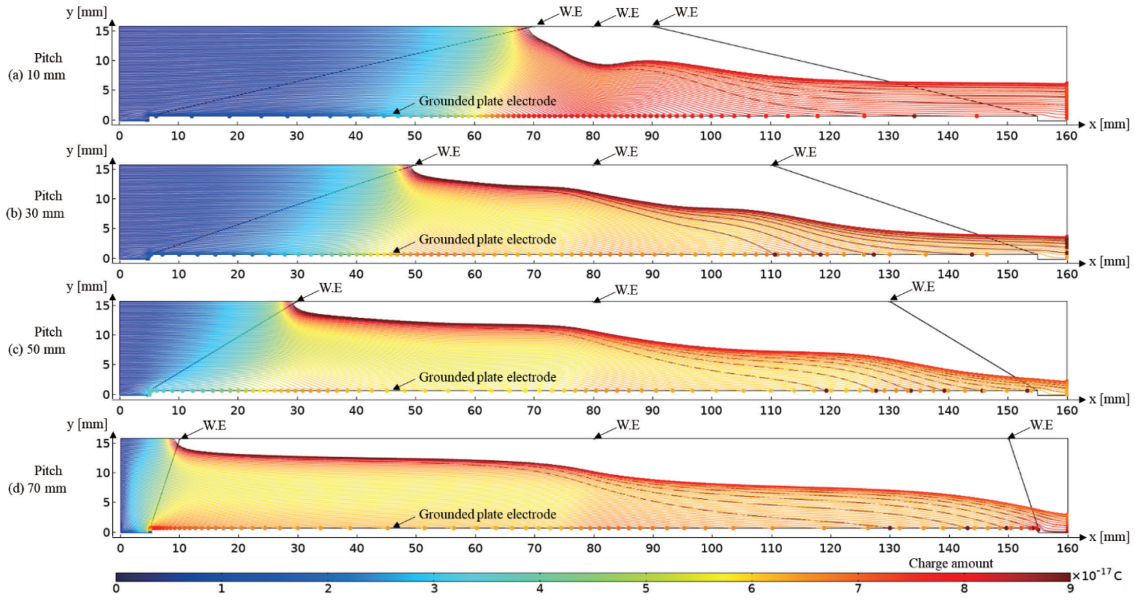

Fig. 6 Particle charge and trajectory at each pitch length.

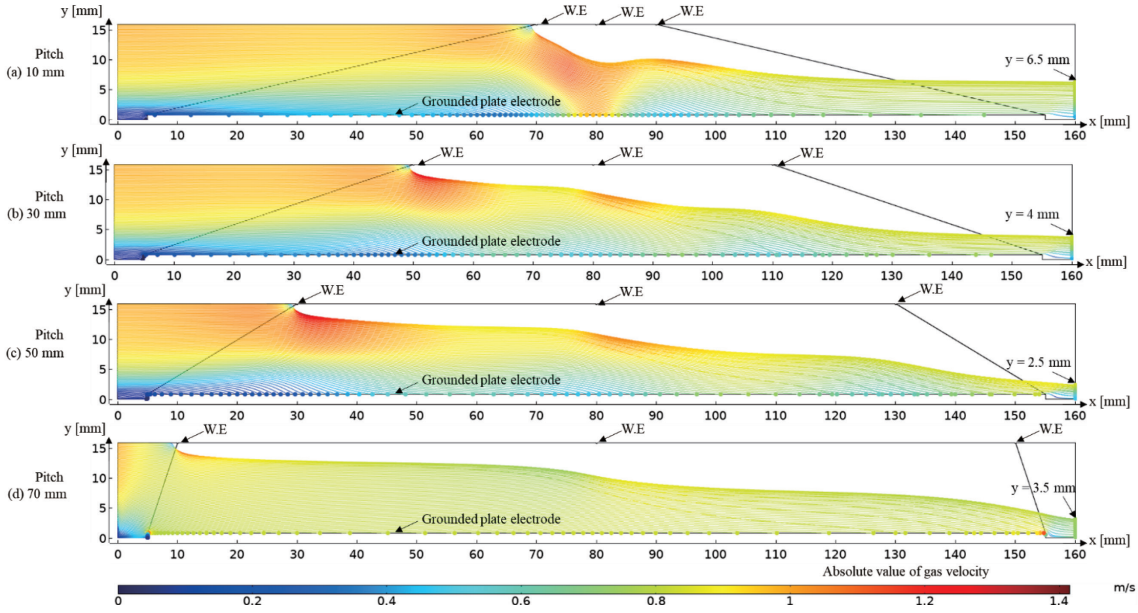

Fig. 7 Particle velocity and trajectory at each pitch length.

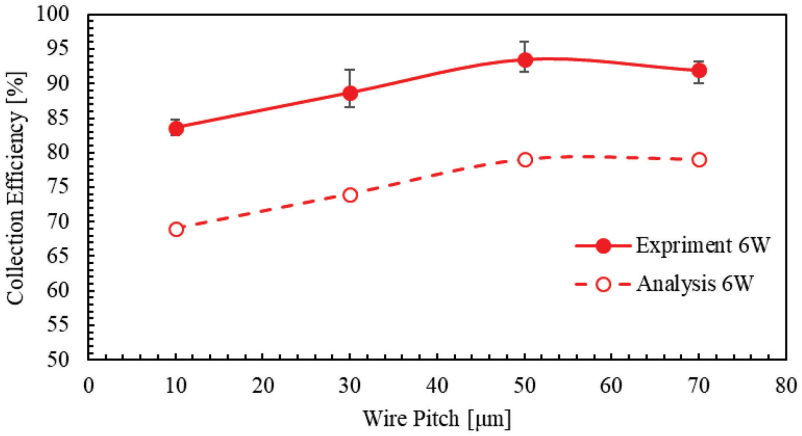

Fig. 8 Relationship between collection efficiency and wire pitch length.

wire electrodes decreased due to the effect of the gas flow distribution as shown in Fig. 5. The average migration velocities, which were the y components of the particle velocities, at the pitch length of 10 mm, 30 mm, 50 mm and 70 mm were -0.0061 m/s, -0.0067 m/s, -0.0070 m/s and -0.0069 m/s, respectively. The average migration velocity at 50 mm was the fastest. This is because the negative ion density and the electric field intensity were relatively uniform distributions, and these average values were the highest as shown in Fig. 3 and 4. Although the particle charge amount was the lowest, the migration velocity increased due to the increase of Coulomb force. In addition, the distance y from the wall at the location x of 160 mm at the pitch length of 50 mm was 2.5 mm, which was the nearest among the calculation conditions.

4.6 Relationship between collection efficiency and pitch length

The relationship between collection efficiency and the pitch length is shown in Fig. 8. The analysis collection efficiency was calculated from equation (1), and the experimental efficiency was from equation (2). The number of experiments is three times, and the error bar indicates minimum and maximum values. The analysis collection efficiency increased as the wire pitch length increased, and saturated at the pitch greater than 50 mm. The analysis efficiencies at the pitch length of 50 mm and 70 mm were the same of 79%. However, as the particles were most attracted toward the grounded plate electrode as described in Fig. 7, it is considered that the pitch length of 50 mm is optimum. The experimental value also increased with increasing the pitch length, and reached 93% at 50 mm and 91% at 70 mm. The experimental collection efficiency became the highest at 50 mm. The experimental values were greater than the analysis values. This is most likely because the governing equations in this study are not considered the particle form, the particle agglomeration, the re-entrainment or the particle distribution, etc. While the analysis collection efficiency was different from the experimental value, the tendency of the analysis result agreed with the experimental result. From these results, it is revealed that the optimum pitch length at the same power consumption is approximately 50 mm at the gap length of 15 mm. In other words, the optimum pitch is approximately 3.2 times the gap length.

5. Conclusion

The optimum pitch length between wires at the same energy consumption in the ESP with multiple wire electrode was investigated using the simulation method, which were revealed the validity. The grounded plate electrode was 150 mm, and the gap distance between wire and the grounded plate electrode was 15 mm. Furthermore, the analysis collection efficiency was compared to the experimental efficiency, and the validity of the analysis result was investigated. The results are follows:

(1) The averages of the negative ion density and the electric field intensity in the analysis area was the highest value in the pitch length of 50 mm.
(2) The average charge amount at the pitch length of 10 mm was the largest, and that at 50 mm was the smallest.
(3) The average migration velocity at the pitch length of 50 mm was the fastest.
(4) The analysis collection efficiency at the pitch length of 50 mm was the same value to that at 70 mm. However, it was considered that the optimum pitch length was 50 mm, as the particles were most attracted to the grounded plate electrode.
(5) Although the value of the analysis collection efficiency was different from experimental value, the tendency in the analysis result agreed with the experimental result.

From these results, it was revealed that the optimum pitch length between wires at the same energy consumption was 50 mm which was approximately 3.2 times the gap length.

References

[1] Zhuohan Li, Cheng Shao, Yi An, Gaofeng Xu, Energy-saving optimal control for a factual electrostatic precipitator with multiple electric-field stages based on GA, Journal of Process Control, Vol. 23, pp. 1041-1051, 2013
[2] B. Liu, Q. Zheng, C. Gao, C. Du, S. Wang, S. Li1, J. Zhang, T. Bao, Y. Yang, J. Wang, P. Han, and K. Yan, Emission Reduction and Energy Saving of Electrostatic Precipitation Used for Coal-fired

Boilers, International Journal of Plasma Environmental Science & Technology, Vol.11, No.2, MARCH 2018, pp. 165-169.
[3] MA Jinhui, YANG Yaowen, WANG Ronghua, YAN Keping, Industrial Applications of a New AVC for Upgrading ESP to Save Energy and Improve Efficiency, Proceeding of 11th International Conference on Electrostatic Precipitation, pp. 281-283, 2008
[4] M. Williamsson , A. Karlsson , N. Dash , P. Ranstad , E. Önnerby Pettersson, Energy optimization in ESP with advanced control system, Proceeding of ICESP 2016
[5] Kjell Porle, Reduced Emission and Energy Consumption with Pulsed Energization of Electrostatic Precipitators, Journal of Electrostatics, Vol. 16, pp. 299-314, 1985
[6] A. Jaworek, A.T. Sobczyk, A. Marchewicz, A. Krupa, T. Czech, Ł. Śliwiński, A. Ottawa, A. Charchalis, Two-stage vs. two-field electrostatic precipitator, Journal of Electrostatics, Vol. 90, pp. 106-112, 2017
[7] Fumio Isahaya, Kizo Otsuka, Experimental and Theoretical Analysis on Gaseous Discharge Characteristics of Electrostatic Precipitator, Hitachi hyoron, Vol. 47, No. 7, pp. 1-8, 1965 (in Japanese)
[8] Y. Deguchi, T. Sugimoto, T. Suzuki, Electrostatic Phenomena in High Temperature Air Gaps (Part 2) - D.C Corona Current and Optimum Conditions for E.P. Operation-, CRIEPI, No. 180073, 1981
[9] Zakariya Al-Hamouz, Amer El-Hamouz, Nabil Abuzaid, Simulation and experimental studies of corona power loss in a dust loaded wire-duct electrostatic precipitator, Advanced Powder Technology, 22, pp.706-714, 2011
[10] Yuying Xu, Baoqing Deng, Haiyan Zhang, Xianpeng Chen, Numerical simulation of electrostatic field and flow field in an electro static precipitator, Journal of Air Pollution and Health, 4(2), pp.87-98, Spring 2019
[11] Yoshihiro Kawada, Hirotaka Shimizu, Akinori Zukeran, Numerical Study of the Suitable Precharger Grounded Electrode Length in Two-Stage-Type Electrostatic Precipitator, IEEE Transactions on Industry Applications, Vol. 55, No.1, pp. 833-839, 2019
[12] Ryota Tamura, Kohei Ito, Yuya Date, Akinori Zukeran, Yoshihiro Kawada, Tomohiro Taoka, Simulation and measurement of particle trajectory in an electrostatic precipitator with multiple wire electrodes, IEEE Transactions on Industry Applications, DOI 10.1109/TIA.2021.3140192, 2022
[13] Kohei ITO, Yuma MORI, Akinori ZUKERAN, Yoshihiro KAWADA, Tomohiro TAOKA, Kenji SHIBATA: Simulation and measurement of ionic flow in a wire-to-plate type electrostatic precipitator, Journal of the Institute Electrostatics Japan, 43 [1] (2018) 25-30 (in Japanese)
[14] Kohei Ito, Ryota Tamura, Akinori Zukeran, Yoshihiro Kawada, Tomohiro Taoka: Simulation and measurement of charged particle trajectory with ionic flow in a wire-to-plate type electrostatic precipitator, Journal of Electrostatics, Vol. 107, September, 2020, doi.org/10.1016/j.elstat.2020.103488

神奈川工科大学研究報告

B–47　理工学編　通巻 47 号

令和 5 年 3 月 1 日　発行

編集兼発行者　神 奈 川 工 科 大 学
〒 243–0292　神奈川県厚木市下荻野1030
電　話　046–241–6221

印　刷　者　株式会社スクールパートナーズ